

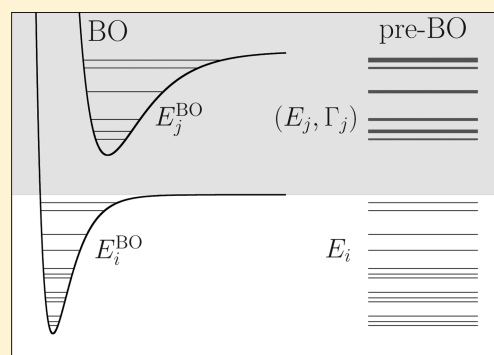
On the Calculation of Resonances in Pre-Born–Oppenheimer Molecular Structure Theory

Edit Mátyus*

Laboratory of Molecular Structure and Dynamics, Institute of Chemistry, Eötvös University, P.O. Box 32, H-1518, Budapest 112, Hungary

S Supporting Information

ABSTRACT: The main motivation for this work is the exploration of rotational–vibrational states corresponding to electronic excitations in a pre-Born–Oppenheimer quantum theory of molecules. These states are often embedded in the continuum of the lower-lying dissociation channel of the same symmetry and thus are thought to be resonances. To calculate rovibronic resonances, the pre-Born–Oppenheimer variational approach of [*J. Chem. Phys.* **2012**, *137*, 024104], based on the usage of explicitly correlated Gaussian functions and the global vector representation, is extended with the complex coordinate rotation method. The developed computer program is used to calculate resonance energies and widths for the three-particle positronium anion, Ps^- , and the four-particle positronium molecule, Ps_2 . Furthermore, the excited bound and resonance rovibronic states of the four-particle H_2 molecule are also considered. Resonance energies and widths are estimated for the lowest-energy resonances of H_2 beyond the $b^3\Sigma_u^+$ continuum.



INTRODUCTION

The present work is devoted to conceptual and computational problems in pre-Born–Oppenheimer (pre-BO) molecular structure theory. Without the Born–Oppenheimer (BO) approximation,^{1–3} in a “pre-BO world”, we can gain in accuracy for the numerical results but lose a central paradigm for the well-accustomed concepts of chemistry. The reconstruction or interpretation of many common chemical concepts becomes a real challenge. One of these famous challenges, the problem of the quantum structure of molecules, has been recognized long ago^{4–7} and studied by many authors.^{8–20}

In the present work we address another challenge, the status of electronically excited rotational–vibrational states in a pre-BO quantum mechanical description. In a pre-BO description there are no electronic states with corresponding potential energy curves or surfaces on which the rotational–vibrational Schrödinger equation could be solved. In addition, rotational–vibrational states corresponding to electronic excitations are often embedded in the lowest-lying dissociation channel of the system (Figure 1) prone to predissociation.²¹ These rovibronic states are thus accessible in a pre-BO description only as resonances. These rovibronic resonances are characterized with some energy and width corresponding to a finite nonradiative (predissociative) lifetime. Our aim is to explore how these properties can be calculated in a pre-BO approach.

As for the numerical results, there are practical approaches used for the calculation of quasi-bound states in molecular science.^{22–24} The stabilization technique, a very simple computational tool, has been used to identify resonances and to estimate the resonance energy^{25–27} and can also be extended

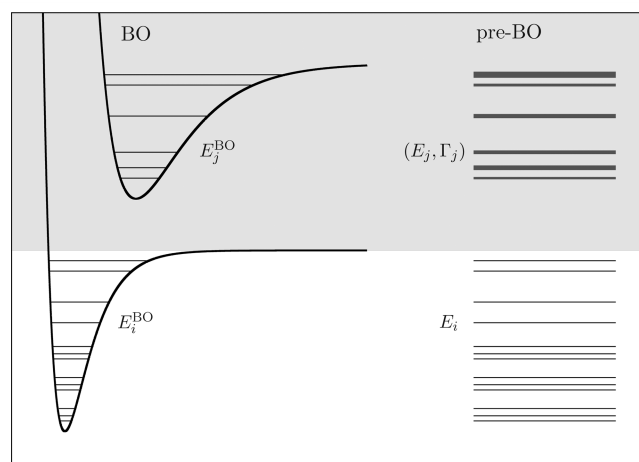


Figure 1. Motivation for this work: calculation of rovibronic levels corresponding to electronically excited states, which are bound in the Born–Oppenheimer description but which appear as resonances in pre-Born–Oppenheimer molecular structure theory.

to the calculations of the width.^{28–31} The complex coordinate rotation method^{32–34} is a neat mathematical approach for the calculation of the resonance energy and width and has been used in several cases,^{23,24} for example in rotational–vibrational

Special Issue: Joel M. Bowman Festschrift

Received: January 30, 2013

Revised: May 11, 2013

Published: May 15, 2013

calculations on a potential energy surface within the Born–Oppenheimer (BO) theory.^{31,35} The usage of complex absorbing potentials^{36–38} has been a popular technique in molecular spectroscopy and quantum reaction kinetics with many applications.^{39–41} There exist also more involved and specialized approaches, such as the solution of the Faddeev–Merkuriev integral equations.^{42,43}

The present work is organized as follows. First, the necessary theoretical framework is described for the variational solution of the Schrödinger equation for bound states of few-particle systems. Then, this approach is extended for the identification and calculation of quasi-bound states. Next, numerical examples are presented for the three-particle Ps^- and the four-particle Ps_2 . Finally, the description of excited bound and resonance rovibronic states of the four-particle H_2 is explored. In the end, we finish with a summary and outlook.

■ THEORY AND COMPUTATIONAL STRATEGY

The Schrödinger equation for an $(n_p + 1)$ -particle system with m_i masses and q_i electric charges assigned to the particles is

$$\hat{H}\Psi = E\Psi \quad (1)$$

with the nonrelativistic quantum Hamiltonian in Hartree atomic units

$$\hat{H} = \hat{T} + \hat{V} = -\sum_{i=1}^{n_p+1} \frac{1}{2m_i} \Delta_{r_i} + \sum_{i=1}^{n_p+1} \sum_{j>i}^{n_p+1} \frac{q_i q_j}{|r_i - r_j|} \quad (2)$$

written in laboratory-fixed Cartesian coordinates $r = (r_1, r_2, \dots, r_{n_p+1})$.

In the present work we use the bound-state variational approach of ref 44 and (a) combine it with the stabilization technique to quickly identify long-lived resonances and (b) extend it with the complex coordinate rotation method to calculate resonance energies and widths.

Variational pre-BO Calculations Using Explicitly Correlated Gaussian Functions and the Global Vector Representation. The overall translation of the center of mass is eliminated by writing the kinetic energy operator in terms of Jacobi Cartesian coordinates, and the translational kinetic energy of the center of mass is subtracted. As an alternative to this approach, the original laboratory-fixed Cartesian coordinates can be used throughout the calculations without any further coordinate transformation employing a special elimination technique for the overall translation during the evaluation of the matrix elements.⁴⁵

The matrix representation of the translationally invariant Hamiltonian is constructed using a symmetry-adapted basis set defined as follows.

A basis function with the quantum numbers $\lambda = (N, M_N, p)$ and $\varsigma = (S_w, M_{S_w}, S_b, M_{S_b}, \dots)$ (a, b, \dots label the particle type) is constructed as

$$\Phi^{[\lambda, \varsigma]}(r, \sigma) = \hat{\mathcal{A}}\{\phi^{[\lambda]}(r)\chi^{[\varsigma]}(\sigma)\} \quad (3)$$

where $\hat{\mathcal{A}} = (N_{\text{perm}})^{-1/2} \sum_{i=1}^{N_{\text{perm}}} \varepsilon_i \hat{P}_i$ is the symmetrization and antisymmetrization operator for bosonic and fermionic-type particles, respectively. \hat{P}_i ($i = 1, 2, \dots, N_{\text{perm}}$) is an operator permuting identical particles, and $\varepsilon_i = -1$ if \hat{P}_i corresponds to an odd number of interchanges of fermions; otherwise, $\varepsilon_i = +1$. (N denotes here the total spatial (orbital plus rotational) angular momentum quantum number in agreement with the

recommendations of the International Union of Pure and Applied Chemistry.⁴⁶ We note that in ref 44 the symbol L was used in the same sense. Furthermore, p is the parity, which we call “natural” if $p = (-1)^N$ and “unnatural” if $p = (-1)^{N+1}$. In this work we restrict the discussion to natural-parity states. The total spin quantum number for particles of type a is S_a . For example, S_p and S_e denote the total spin quantum numbers for the protons and the electrons, respectively.)

The spatial part of the basis functions with natural parity, $p = (-1)^N$, is constructed using explicitly correlated Gaussian functions^{47–51} and the global vector representation^{52–54} as

$$\phi^{[\lambda]}(r; \alpha, u, K) = |\nu|^{2K+N} Y_{NM_N}(\hat{\nu}) \exp\left(-\frac{1}{2} \sum_{i=1}^{n_p+1} \sum_{j>i}^{n_p+1} \alpha_{ij}(r_i - r_j)^2\right) \quad (4)$$

where the $\hat{\nu} = \nu/|\nu|$ unit vector points in the direction of the global vector, $\nu = \sum_{i=1}^{n_p+1} u_i^{(0)} r_i$. Y_{NM_N} denotes the N th order M_N th degree spherical harmonic function. The spin function, $\chi^{[\varsigma]}$, is constructed from elementary spin functions so that the resulting function is an eigenfunction of \hat{S}_a^2 and $(\hat{S}_a)_z$ for each type of particles (a, b, \dots) with the quantum numbers $\varsigma = (S_w, M_{S_w}, S_b, M_{S_b}, \dots)$.

Then, the resulting $\Phi^{[\lambda, \varsigma]}$ basis function has the quantum numbers of the nonrelativistic quantum theory (it is “symmetry-adapted”) and contains free parameters, which can be optimized for an efficient description of the “internal structure” of a system. The free parameters of the spatial function, eq 4, are K ; α , α_{ij} ($i = 1, \dots, n_p + 1$, $j = i + 1, \dots, n_p + 1$); and u , $u_i^{(0)}$ ($i = 1, \dots, n_p + 1$) with the restriction $\sum_{i=1}^{n_p+1} u_i^{(0)} = 0$, which guarantees translational invariance. The spin functions used in this work do not contain any free parameters.

We only note here that for the positronium molecule, Ps_2 , as a special case studied in this work, the entire basis function was additionally adapted to the charge-conjugation symmetry of the electrons and the positrons.^{55–57}

The matrix elements of the kinetic and potential energy operators corresponding to the basis functions with natural parity, eqs 3 and 4, were evaluated with the pre-BO program according to ref 44.

Since the basis functions are not orthogonal we have to solve a generalized eigenvalue problem

$$Hc_i = E_i S c_i \quad (5)$$

to find the variationally optimal linear combination of the basis functions with the linear combination coefficients c_i corresponding to the eigenvalue E_i . The generalized eigenproblem is solved by introducing $H' = S^{-1/2} H S^{-1/2}$ and $c'_i = S^{1/2} c_i$, which simplifies the eigenvalue equation, eq 5, to $H'c'_i = E_i c'_i$. In our computations the Cholesky decomposition of S for the evaluation of $S^{-1/2}$ as well as the diagonalization of the real, symmetric transformed Hamiltonian matrix, H' , were carried out by using the LAPACK library routines.⁵⁸

The computational efficiency and usefulness of the variational approach described depend on the parametrization of the basis functions (the choice of the values of K , α , and u_i for the basis functions $I = 1, \dots, N_b$). For bound-state calculations we adopted the stochastic variational approach^{54,59–62} for the optimization of the basis function parameters. The (quasi-)optimization of the parameter set is a very delicate problem, and our recipe includes the following details:⁴⁴ (a) a system-

Table 1. Identified Bound- and Resonance-State Energies and Resonance Widths, in E_h , of $\text{Ps}^- = \{e^-, e^-, e^+\}^a$

| $(N, p, S_-)^b$ | $\text{Re}(\mathcal{E})^c$ | $\Gamma/2^c$ | $\text{Re}(\mathcal{E}_{\text{ref}})^d$ | $\Gamma_{\text{ref}}/2^d$ | ref |
|-----------------|-----------------------------|------------------------|-----------------------------------------|---------------------------|-----|
| (0,+1,0) | -0.262 005 070 ^e | 0 ^e | -0.262 005 070 | 0 | 66 |
| (0,+1,0) | -0.076 030 455 | 2.152×10^{-5} | -0.076 030 442 | 2.1517×10^{-5} | 64 |
| (0,+1,0) | -0.063 649 173 | 4.369×10^{-6} | -0.063 649 175 | 4.3393×10^{-6} | 64 |
| (0,+1,0) | -0.062 609 | 2.5×10^{-5} | -0.062 550 | 5.0×10^{-7} | 42 |
| (0,+1,0) | -0.035 341 85 | 3.730×10^{-5} | -0.035 341 885 | 3.7329×10^{-5} | 64 |
| (0,+1,0) | -0.029 845 70 | 2.781×10^{-5} | -0.029 846 146 | 2.6356×10^{-5} | 64 |
| (0,+1,0) | -0.028 271 | 1.8×10^{-5} | -0.028 200 | 7.5×10^{-6} | 42 |
| (0,+1,0) | -0.020 199 | 8.800×10^{-5} | -0.020 213 921 | 6.5026×10^{-5} | 64 |
| (0,+1,1) | -0.063 537 352 | 2.132×10^{-9} | -0.063 537 354 | 1.5700×10^{-9} | 64 |
| (0,+1,1) | -0.062 591 | 2.6×10^{-7} | -0.062 550 | 2.5×10^{-10} | 42 |
| (0,+1,1) | -0.029 369 87 | 1.300×10^{-7} | -0.029 370 687 | 9.3950×10^{-8} | 64 |
| (0,+1,1) | -0.028 21 | 1.9×10^{-5} | -0.028 05 | 5.0×10^{-8} | 42 |
| (0,+1,1) | -0.017 071 | 6.710×10^{-6} | -0.017 101 172 | 3.5609×10^{-7} | 42 |

^aThe dissociation threshold energies, in E_h , accessible for both the $S_- = 0$ and 1 states are $E(\text{Ps}(1)) = -1/4 = -0.25$, $E(\text{Ps}(2)) = -1/16 = -0.0625$, and $E(\text{Ps}(3)) = -1/36 = -0.0277$. ^b N , p , and S_- : total spatial angular momentum quantum number, parity, and total spin quantum number of the electrons, respectively. ^c $\text{Re}(\mathcal{E})$ and Γ : resonance energy and width with $\Gamma/2 = -\text{Im}(\mathcal{E})$ calculated in this work. ^d $\text{Re}(\mathcal{E}_{\text{ref}})$ and Γ_{ref} : resonance energy width with $\Gamma_{\text{ref}}/2 = -\text{Im}(\mathcal{E}_{\text{ref}})$ taken from refs 42 and 64. ^eBound state.

adapted random number generator is constructed using a sampling-importance resampling strategy for the generation of trial parameter sets; (b) the acceptance criterion of the generated trial values is based on the linear independence condition and the energy minimization requirement (relying on the variational principle); (c) the selected parameters are fine-tuned using a simple random walk approach or Powell's method.⁶³

Furthermore, once a parameter set has been selected or optimized for a system with some quantum numbers, it can be used, "transferred", to parametrize basis functions for the same system with different quantum numbers ("parameter transfer approach"). It is important to emphasize that the basis functions are not transferred since they have a different mathematical form for different quantum numbers, but only the parameter set is taken over from one calculation to another.

Calculation of Resonances. The bound-state pre-BO approach described was extended for the calculation of resonance states as follows. First of all, without any change of the computer program, we looked for the quasi-stabilization of higher-energy eigenvalues (higher than the lowest-energy threshold) of the real eigenvalue problem. This application of the stabilization technique^{25–27} is a simple, practical test for identifying possible quasi-bound states and was found to be useful as a first check of the higher-energy eigenspectrum. By making full use of the stabilization theory, both the resonance energies and widths could be calculated from consecutive diagonalization of the (real) Hamiltonian matrix corresponding to increasing number of basis functions, which cover increasing boxes of the configuration space.^{28–31}

Instead of using this approach, the complex coordinate rotation method (CCRM)^{23,24,32–34} was implemented for the calculation of resonance parameters, energies, and widths. The resonance parameters were determined by identifying stabilization points in the complex plane with respect to the coordinate rotation angle and (the size and parametrization of) the basis set. The localized real part of the eigenvalue, $\text{Re}(\mathcal{E})$, was taken to be the resonance energy, and the imaginary part provided the resonance width, $\Gamma = -2\text{Im}(\mathcal{E})$, which is inversely proportional to the lifetime, $\tau = \hbar/\Gamma$.²²

Implementation of the Complex Coordinate Rotation Method for the Coulomb Hamiltonian. The complex

scaling of the coordinates $r \rightarrow re^{i\theta}$ translates to the replacement of the Hamiltonian $\hat{H} = \hat{T} + \hat{V}$ with

$$\hat{\mathcal{H}}(\theta) = e^{-2i\theta}\hat{T} + e^{-i\theta}\hat{V} \quad (6)$$

The matrix representation of $\hat{\mathcal{H}}(\theta)$ is constructed with the matrices of \hat{T} and \hat{V} evaluated by the pre-BO program.⁴⁴ Then, the eigenvalue equation for $\hat{\mathcal{H}}(\theta)$ reads as

$$\mathcal{H}(\theta)v_i(\theta) = \mathcal{E}_i(\theta)Sv_i(\theta) \quad (7)$$

where S is the overlap matrix of the (linearly independent) set of basis functions. S is eliminated from the equation similarly to the case of the real generalized eigenproblem, eq 5

$$\mathcal{H}'(\theta)v'_i(\theta) = \mathcal{E}_i(\theta)v'_i(\theta) \quad (8)$$

with

$$\begin{aligned} \mathcal{H}'(\theta) &= e^{-2i\theta}T' + e^{-i\theta}V' \\ &= \cos(2\theta)T' + \cos(\theta)V' - i(\sin(2\theta)T' \\ &\quad + \sin(\theta)V') \end{aligned} \quad (9)$$

and

$$T' = S^{-1/2}TS^{-1/2} \text{ and } V' = S^{-1/2}VS^{-1/2} \quad (10)$$

The complex symmetric eigenvalue problem, eq 8, is solved using the LAPACK library routines.⁵⁸

NUMERICAL RESULTS

The first numerical applications of our implementation were carried out for the notoriously nonadiabatic positronium anion, $\text{Ps}^- = \{e^-, e^-, e^+\}$, and for the positronium molecule, $\text{Ps}_2 = \{e^-, e^-, e^+, e^+\}$. The reason for the choice of these systems was of technical nature: we observed in bound-state calculations⁴⁴ that it was straightforward to find an appropriate parametrization of the basis set for the positronium complexes. Furthermore, comparison of the results with earlier calculations^{27,42,64,65} allowed us to check the developed computational methods and gain experience in the localization of the real and imaginary parts of the complex eigenvalues using the complex coordinate rotation method.

Table 2. Identified Bound- and Resonance-State Energies and Resonance Widths, in E_h , of $Ps_2 = \{e^-, e^-, e^+, e^+\}^a$

| $(N, p, c)^b$ | $(S_-, S_+)^c$ | $Re(\mathcal{E})^d$ | $\Gamma/2^d$ | $Re(\mathcal{E}_{ref})^e$ | $\Gamma_{ref}/2^e$ | ref. |
|------------------|----------------|---------------------------------|-----------------------|---------------------------|-----------------------|------|
| (0,+1,+1) | (0,0) | -0.516 003 789 741 ^f | 0 ^f | -0.516 003 790 416 | 0 | 69 |
| (0,+1,+1) | (0,0) | -0.329 38 | 3.03×10^{-3} | -0.329 4 | 3.1×10^{-3} | 65 |
| (0,+1,+1) | (0,0) | -0.291 7 | 2.5×10^{-3} | -0.292 4 | 1.95×10^{-3} | 65 |
| (0,+1,-1) | (0,0) | -0.314 677 072 ^f | 0 ^f | -0.314 673 3 | 0 | 65 |
| (0,+1,-1) | (0,0) | -0.289 789 3 | 7.7×10^{-5} | -0.289 76 | 7×10^{-5} | 65 |
| (0,+1,-1) | (0,0) | -0.279 25 | 2.3×10^{-4} | -0.279 13 | 1×10^{-4} | 65 |
| (0,+1,+1) | (1,1) | -0.277 2 | 5.4×10^{-4} | -0.276 55 | 1.55×10^{-4} | 65 |
| (0,+1,-1) | (1,1) | -0.309 0 | 5.7×10^{-3} | -0.308 14 | 1.2×10^{-4} | 65 |
| (0,+1,-1) | (1,1) | -0.273 3 | 2.3×10^{-3} | -0.273 6 | 8.5×10^{-4} | 65 |
| (0,+1, ± 1) | (1,0)/(0,1) | -0.330 287 505 ^f | 0 ^f | -0.330 276 81 | 0 | 65 |
| (0,+1, ± 1) | (1,0)/(0,1) | -0.294 3 | 3.1×10^{-3} | -0.293 9 | 2.15×10^{-3} | 65 |
| (0,+1, ± 1) | (1,0)/(0,1) | -0.282 | 2×10^{-3} | -0.282 2 | 8.5×10^{-4} | 65 |

^aFor the five symmetry blocks with different (N, p, c) quantum numbers and (S_-, S_+) labels the lowest accessible thresholds are $Ps(1S) + Ps(1S)$, $Ps(1S) + Ps(2P)$, $Ps(1S) + Ps(2P)$, $Ps(1S) + Ps(1S)$, and $Ps(1S) + Ps(2S,2P)$, respectively.⁶⁸ The corresponding energies, in E_h , are $E(Ps(1) + Ps(1)) = -1/2 = -0.5$ and $E(Ps(1) + Ps(2)) = -5/16 = -0.312 5$. ^b N, p , and c : total spatial angular momentum quantum number, parity, and charge-conjugation quantum number, respectively. ^c S_- and S_+ : total spin quantum numbers for the electrons and the positrons, respectively. In the last symmetry block, $(S_-, S_+) = (0, 1)$ and $(S_-, S_+) = (1, 0)$ are not good quantum numbers because these spin states are coupled due to the charge-conjugation symmetry of the Hamiltonian. ^d $Re(\mathcal{E})$ and Γ : resonance energy and width with $\Gamma/2 = -Im(\mathcal{E})$ calculated in this work. ^e $Re(\mathcal{E}_{ref})$ and Γ_{ref} : resonance energy and width with $\Gamma_{ref}/2 = -Im(\mathcal{E}_{ref})$ taken from ref 65. ^fBound states.

While for the bound-state calculations the basis function parameters were optimized for the lowest-energy level(s) using the variational principle, this handy optimization criterion was not available in the CCRM calculations. Thus, we used optimized bound-state basis sets and enlarged them with linearly independent basis functions for the estimation of the resonance parameters.

Next, we investigated the calculation of some of the excited states of the H_2 molecule. The construction of a reasonably good parametrization for the basis set has turned out to be a challenge. Nevertheless, we describe the essence of our observations and give calculated resonance energy values and approximate widths for the lowest-lying excited states beyond the $b^3\Sigma_u^+$ repulsive electronic state embedded in the $H(1) + H(1)$ continuum.

Ps^- . In Table 1 bound- and resonance-state parameters ($N = 0, p = +1$) are collected, which were obtained in this work. The basis sets were generated using the energy minimization and the linear independence conditions using a random number generator setup following the strategy described in ref 44. The parameters for the largest basis sets used during the calculations are given in the Supporting Information. The generated basis sets were apparently large and flexible enough to obtain resonance states not only beyond the first but also beyond the second and the third dissociation channels which correspond to $Ps(1) + e^-$, $Ps(2) + e^-$, and $Ps(3) + e^-$, respectively. As to the accuracy, the (real) variational principle, directly applicable for bound states, is not useful for the assessment of the resonance parameters. Instead, we used benchmarks available in the literature resulting from extensive three-body calculations using Pekeris-type wave functions with one and two length scales⁶⁴ and from the solution of the Fadeev–Merkuriev integral equations for three-body systems.⁴²

First of all, the present results and the literature data are in satisfactory agreement. Our results could be certainly improved by running more extensive calculations with larger basis sets. Instead of going in this direction, a careful comparison is carried out with the reference data to learn about the accuracy and convergence behavior of our approach. The results are often in excellent agreement with the benchmarks, but in some

cases the lifetimes are orders of magnitude off. It can be observed that the calculated lifetimes are worse when the real part of the complex energy was determined less accurately (and given to less significant digits in Table 1). The inaccuracy appears in both the real and the imaginary parts and is about of the same order of magnitude compared to the absolute value of the complex energy. Thus, if the widths are expected to be very small and the real part can be determined only to a few digits, the width should be considered only as a rough estimate to its exact value. This observation can be used later in this work also for the assessment of the calculations carried out for the four-particle Ps_2 and H_2 .

Ps_2 . Our next test case was the four-particle positronium molecule, $Ps_2 = \{e^-, e^-, e^+, e^+\}$. Resonances of the positronium molecule have recently attracted attention.^{27,65,67} Ps_2 has few bound states, and thus a detailed spectroscopic investigation of its structure and dynamics is possible only through the detection and analysis of its quasi-bound states.

In our list of numerical examples, the positronium molecule is unique because, in addition to the spatial symmetries, its Hamiltonian is invariant under the conjugation of the electric charges. To account for this additional property, the basis functions, eqs 3 and 4, were adapted also to the charge conjugation symmetry.^{55–57,65,68} As a result, the total symmetry-adapted basis functions and also the calculated wave functions are not necessarily eigenfunctions for the total spin angular momentum of the electrons or that of the positrons, \hat{S}_-^2 or \hat{S}_+^2 . Nevertheless, the total spatial angular momentum quantum number, N , the parity, p , as well as the charge-conjugation parity, $c = +1$ or -1 , are always good quantum numbers.

The parametrization strategy of the basis set was similar to that used for Ps^- : we employed (a) the energy minimization condition for the lowest-energy eigenvalue and (b) the linear independence condition for the generation of new basis function parameters. The parameter sets used in the largest calculations are given in the Supporting Information.

The bound and resonance states calculated with $N = 0$ total spatial angular momentum quantum number and $p = +1$ parity are collected in Table 2. Considering all possible charge

conjugation and spin functions, we obtained only three bound states in agreement with the literature.^{27,65,69} Two of the three calculated bound states substantially improve on the best available results.⁶⁵ It is interesting to note that the bound state with $E = -0.314\,677\,072\,E_h$ ($c = -1$ and $(S_-, S_+) = (1, 1)$) is bound only due to the charge-conjugation symmetry of the electrons and the positrons. The localization of the energy and width for the lowest-energy resonance state of Ps_2 is shown in Figure 2. The calculated resonance positions are in good

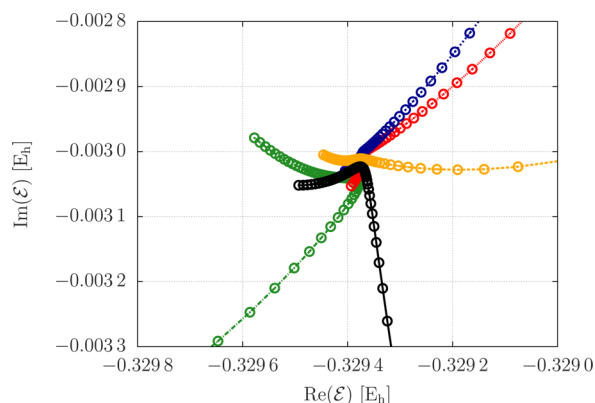


Figure 2. Localization of the parameters for the lowest-energy resonance state of Ps_2 with $N = 0$, $p = +1$, $c = +1$, and $S_- = 0$, $S_+ = 0$. The stabilization of the trajectories with respect to the rotation angle (circles) and the basis functions (colors) is shown. The stabilization point is located at $(\text{Re}(\mathcal{E}), \text{Im}(\mathcal{E})) = (-0.329\,38, -0.003\,03)\,E_h$.

agreement with the literature. In some cases our results might even improve on the best available data,^{27,65} although there is no such direct criterion for the assessment of the accuracy of the resonance parameters as the variational principle for bound states.

Toward the Calculation of Rovibronic Resonances of H_2 . Next, our goal was to explore how the lowest-lying resonance states of H_2 can be calculated in a pre-Born–Oppenheimer quantum mechanical approach. It could be anticipated that one of the major challenges in this undertaking would be the parametrization of the basis functions, which was already in the bound-state calculations more demanding for H_2 than for Ps_2 .⁴⁴ In the bound-state calculations the optimized parameters were fine-tuned in repeated cycles. The entire parameter selection and optimization procedure relied on the variational principle and the minimization of the energy.

According to the spatial and permutational symmetry properties of the H_2 molecule, there are four different blocks with natural parity

$$\text{B1: } "X^1\Sigma_g^+ \text{ block}": N \geq 0, p = (-1)^N,$$

$$S_p = (1 - p)/2, S_e = 0$$

$$\text{B2: } "B^1\Sigma_u^+ \text{ block}": N \geq 0, p = (-1)^N,$$

$$S_p = (1 + p)/2, S_e = 0$$

$$\text{B3: } "a^3\Sigma_g^+ \text{ block}": N \geq 0, p = (-1)^N,$$

$$S_p = (1 - p)/2, S_e = 1$$

$$\text{B4: } "b^3\Sigma_u^+ \text{ block}": N \geq 0, p = (-1)^N,$$

$$S_p = (1 + p)/2, S_e = 1$$

which can be calculated in independent runs with our computer program using basis functions with the appropriate quantum numbers, eqs 3 and 4. The lowest-energy levels of the first three blocks correspond to bound states, while the last block starts with the $\text{H}(1) + \text{H}(1)$ continuum. In the BO picture the $b^3\Sigma_u^+$ electronic state is repulsive⁷⁰ and does not support any bound rotational–vibrational levels (see Figure 3 and Table 3). Then, one of our goals was the identification of the lowest-energy quasi-bound states in the $b^3\Sigma_u^+$ block.

During the calculation of the lowest-energy resonances of Ps_2 , the basis function parameters were generated randomly using a system-adapted random number generator.⁴⁴ Unfortunately, this simple strategy for the H_2 resonances was not useful.

The energy minimization criterion for the lowest (few) eigenstates was not useful either since it resulted only in the accumulation of functions near the $\text{H}(1) + \text{H}(1)$ limit, the lowest-energy levels in the $b^3\Sigma_u^+$ block, and the higher-lying quasi-bound states were not at all described by the basis sets generated in this way.

Then, our alternative working strategy was the usage of the parameter transfer approach (described in Section “Theory and Computational Strategy” and in ref 44). In this approach a parameter set optimized for a bound state with some quantum numbers, “state \mathcal{A} ”, is used to parametrize the basis functions corresponding to another set of quantum numbers and used to calculate “state \mathcal{B} ”. It is important to emphasize that the mathematical form of the basis functions is defined by the selected values of the quantum numbers, eqs 3 and 4, and thus not the basis functions but only the parameters are transferred from one calculation to another. Our qualitative understanding tells us that this parameter-transfer strategy is computationally useful if the internal structures of state \mathcal{A} and state \mathcal{B} are more or less similar. By inspecting the orientation chart of H_2 (Figure 3), our idea was that the combination of the (natural-parity) bound-state optimized parameter sets could provide a parametrization good enough for the identification of the lowest-lying resonance states embedded in the $b^3\Sigma_u^+$ continuum.

For this purpose, we used the parameters of 2250 basis functions optimized for the lowest-lying bound states with $N = 0$ and 1 angular momentum quantum number corresponding to the $X^1\Sigma_g^+$, $B^1\Sigma_u^+$, and $a^3\Sigma_g^+$ blocks using the sampling-importance resampling strategy of ref 44 and Powell’s method⁶³ for the fine-tuning of each basis function. As a result of these calculations, we obtained a parameter set large enough for $6 \times 2250 = 13\,500$ basis functions. In addition, 1000 basis functions were generated and less tightly optimized for the lowest-energy levels of the $b^3\Sigma_u^+$ block with $N = 0$ and 1. Using this large parameter set, \mathcal{P}_L , 15 500 basis functions were constructed for all possible quantum numbers of the four blocks, B1–B4, with $N = 0, 1$, and 2. In each case the resulting basis set was found to be linearly independent. The complete parameter set is given in the Supporting Information. The proton–electron ratio was $m_p/m_e = 1836.15267247$ throughout the calculations.⁷¹

Bound-State Energy Levels. The lowest-lying energy values obtained with \mathcal{P}_L for the different quantum numbers are collected in Table 3 and are in good agreement with the best available nonrelativistic results in the literature. The energy values of the $X^1\Sigma_g^+$ electronic and vibrational ground states

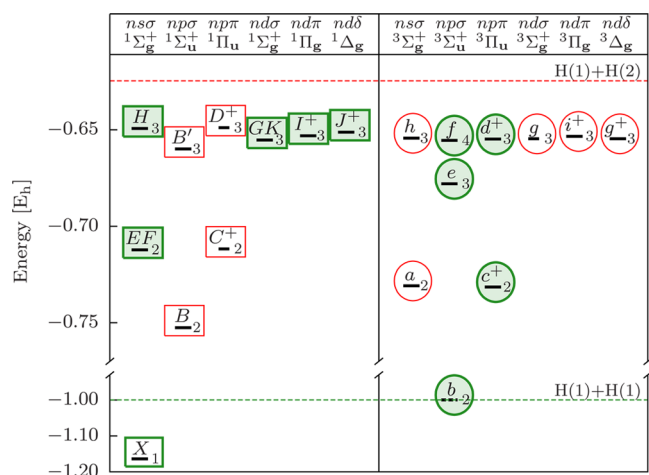


Figure 3. Orientation chart for the electronic states of H_2 below the $H(1) + H(2)$ dissociation threshold (see, for example, Herzberg⁷⁸ or Brown and Carrington⁷⁹). The same color (red or green) and shape (rectangle or ellipse) coding indicates those states, which can be obtained in the same pre-Born–Oppenheimer calculation. Empty objects indicate bound states, while filled objects refer to the fact that the corresponding rovibronic states (if there are any) are resonances embedded in the $H(1) + H(1)$ continuum.

Table 3. Assessment of the Basis Set Parameterization: The Lowest-Lying Bound-State Energies

| $(N, p, S_p, S_e)^a$ | E/E_h^b | $\Delta E_{\text{ref}}/\mu E_h^c$ | ref | assignment ^d |
|----------------------|-------------------------------|-----------------------------------|----------|-------------------------|
| (0,+1,0,0) | −1.164 025 030 | −0.000 6 | 72 | $X^1\Sigma_g^+$ |
| (1,−1,1,0) | −1.163 485 171 | −0.001 4 | 72 | $X^1\Sigma_g^+$ |
| (2,+1,0,0) | −1.162 410 408 | −0.001 9 | 72 | $X^1\Sigma_g^+$ |
| (0,+1,1,0) | −0.753 027 186 | 1.383 7 | 73 | $B^1\Sigma_u^+$ |
| (1,−1,0,0) | −0.752 850 233 | 1.444 6 | 73 | $B^1\Sigma_u^+$ |
| (1,+1,1,0) | −0.752 498 022 | 1.529 1 | 73 | $B^1\Sigma_u^+$ |
| (0,+1,0,1) | −0.730 825 193 | −0.006 9 | 77 | $a^3\Sigma_g^+$ |
| (1,−1,1,1) | −0.730 521 418 | 0.008 0 | 77 | $a^3\Sigma_g^+$ |
| (2,+1,0,1) | −0.729 916 268 | 0.047 9 | 77 | $a^3\Sigma_g^+$ |
| (0,+1,1,1) | [−0.999 450 102] ^e | [−5.578] | <i>f</i> | $b^3\Sigma_u^+$ |
| (1,−1,0,1) | [−0.999 445 835] ^e | [−9.844] | <i>f</i> | $b^3\Sigma_u^+$ |
| (2,+1,1,1) | [−0.999 439 670] ^e | [−16.010] | <i>f</i> | $b^3\Sigma_u^+$ |

^a N : total spatial angular momentum quantum number; p : parity, $p = (-1)^N$; S_p and S_e : total spin quantum numbers for the protons and the electrons, respectively. ^b E : the energy obtained with the largest parameter set, \mathcal{P}_L , used in this study corresponding to 15 500 basis functions for each set of quantum numbers (see the text for details and the Supporting Information for the numerical values). The proton–electron ratio was $m_p/m_e = 1836.152\,672\,47$.⁷¹ ^c $\Delta E_{\text{ref}} = E_{\text{ref}} - E$ with E_{ref} being the best available non-Born–Oppenheimer theoretical energy value in the literature. ^dBorn–Oppenheimer electronic state label. Each energy level given here can be assigned to the lowest-energy vibrational level of the electronic state. ^eThe lowest-energy eigenvalue of the Hamiltonian obtained for the given set of quantum numbers. ^fThe nonrelativistic energy of two ground-state hydrogen atoms, $E(H(1) + H(1)) = -0.999\,455\,679\,E_h$, was used as reference.

with $N = 0, 1$, and 2 are larger by only less than $2\,nE_h$ than the theoretical results of ref 72.

For all three calculated $B^1\Sigma_u^+$ $N = 0, 1, 2$ levels our energy values are lower by more than $1\,\mu E_h$ compared to the results of ref 73 obtained in close-coupling calculations using adiabatic potential energy curves and nonadiabatic couplings for six electronic states. We also note that for the $N = 0$ lowest-lying vibrational level of $B^1\Sigma_u^+$ there is a “variational-perturbational”

estimate given in Table 3 of ref 73, which was anticipated to be more accurate, and thus it was the recommended value for this level in the article, though not a strict upper bound to the exact value. It was obtained not in the six-state close-coupling calculation, but as a result of two-state close-coupling calculations with the potentials and couplings of ref 73, incremented with a nonadiabatic correction term.⁷⁴ This term value translates to the energy value $-0.753\,026\,440\,E_h$ based on the explanation given below eq 13 of ref 73. An earlier nonadiabatic estimate⁷⁵ (not upper bound) for this energy level was $-0.753\,027\,31\,E_h$ calculated using the adiabatic energy and a correction to the BO potential⁷⁶ incremented by a nonadiabatic correction.⁷⁴ For comparison, the pre-Born–Oppenheimer energy calculated in the present work (in a fully variational procedure) is $-0.753\,027\,186\,E_h$ (Table 3).

In the case of the $a^3\Sigma_g^+$ $N = 1, 2$ energy levels the presented energy values obtained in this work are lower than the lowest energies values published.⁷⁷

On the basis of this overview, we can conclude that the parameter set, \mathcal{P}_L , performs well for the lowest-lying bound-state energy levels and also contains basis functions optimized for an approximate description of the $H(1) + H(1)$ continuum. Then, we can hope that the application of this parameter set in the CCRM calculations for the description of the related or just energetically nearby-lying quasi-bound states will be useful.

Electronically Excited Bound and Resonance Rovibronic States. In the orientation chart of H_2 (Figure 3), the electronic states are collected below the $H(1) + H(2)$ dissociation threshold known from the literature^{78,79} (only natural-parity states are considered). Although in our calculations there are no potential energy curves corresponding to electronic states, these conventional electronic-state labels help the orientation and the reference to the calculated energy levels. In the figure those states which are coupled by symmetry and calculated in the same block are highlighted similarly (green or red color and oval or rectangular marking) corresponding to the B1–B4 blocks introduced earlier in this section. This coupling is included in the calculations automatically by specifying the total spatial (orbital plus rotational) angular momentum, parity, and spin quantum numbers. The empty ellipses and rectangles indicate bound states, while the shaded signs are for resonance states embedded in their corresponding lowest-lying continuum (here: $H(1) + H(1)$).

We carried out calculations in all four blocks, B1–B4, with $N = 0, 1$, and 2 total spatial angular momentum quantum numbers, and most of the states indicated in Figure 3 could have been identified using the largest parameter set, \mathcal{P}_L . Unfortunately, the accuracy of the calculated energies often did not meet the level of spectroscopic accuracy,⁸⁰ and thus we collect here only the essence of the calculations.

First of all, the most important qualitative results can be explained by inspecting Figure 4 prepared for the “ $X^1\Sigma_g^+$ block” and for the “ $b^3\Sigma_u^+$ block”, B1 and B4. Figure 4 shows a part of the eigenspectrum of the complex scaled Hamiltonian, $\mathcal{H}(\theta)$ of eq 6, corresponding to small θ values, $\theta \in [0.005, 0.065]$, and the $[-1.2, -0.5]\,E_h$ interval of the real part of the eigenvalues.

In both cases the onset of the $H(1) + H(1)$ continuum can be observed on the real axes at $-0.999\,455\,679\,E_h$. In the $X^1\Sigma_g^+$ block the bound rovibrational energy levels assignable to the $X^1\Sigma_g^+$ electronic state line up on the real axis with $\text{Im}(\mathcal{E}) = 0$ (deviations from this value are due to the

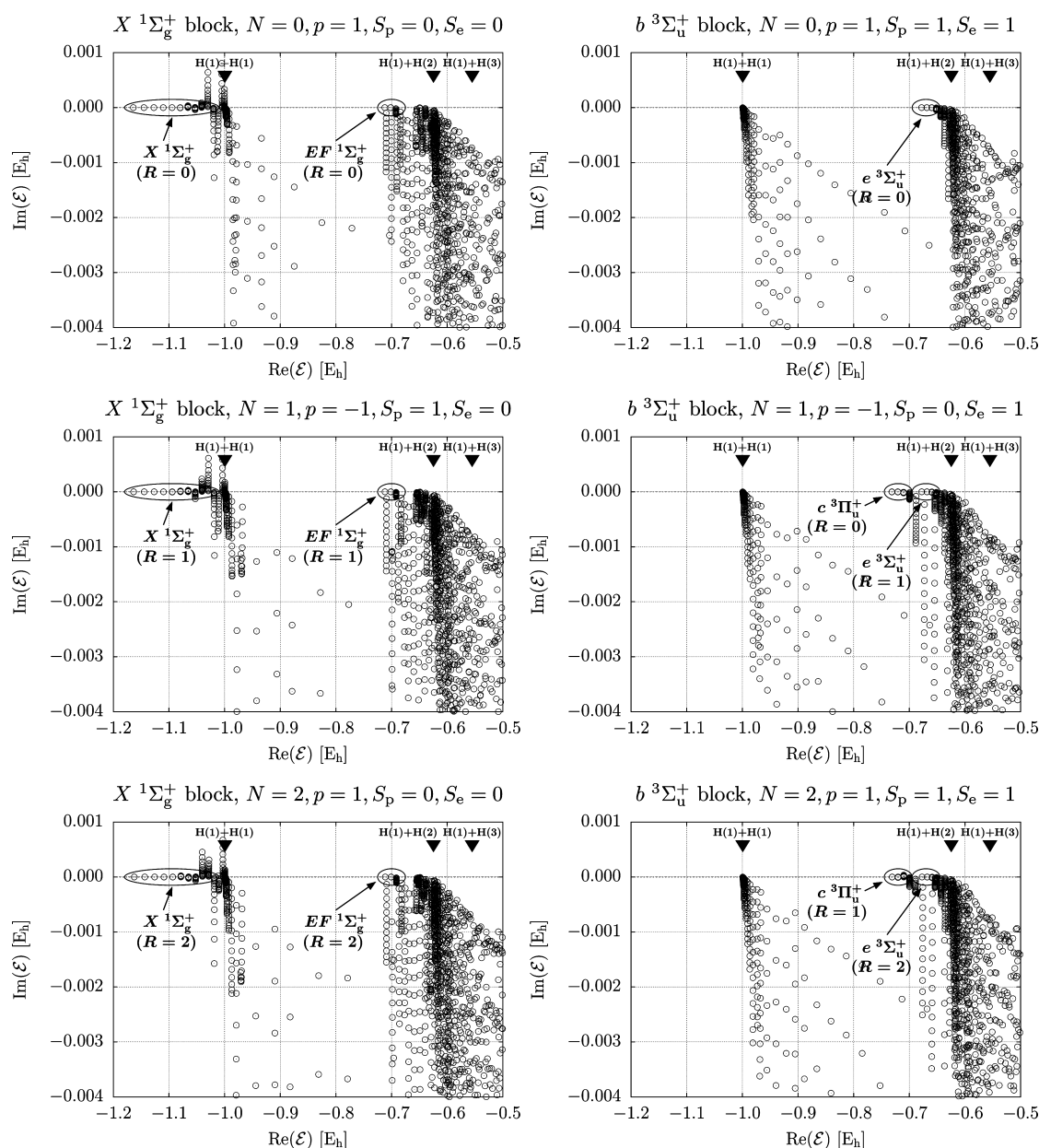


Figure 4. Part of the spectrum of the complex scaled Hamiltonian, $\mathcal{H}(\theta)$, with $\theta \in [0.005, 0.065]$ corresponding to the largest basis set used in this work for the $X^1\Sigma_g^+$ block [$p = (-1)^N$, $S_p = (1-p)/2$, $S_e = 0$] and for the $b^3\Sigma_u^+$ block [$p = (-1)^N$, $S_p = (1+p)/2$, $S_e = 1$] with $N = 0, 1$, and 2 total spatial angular momentum quantum numbers. The black triangles indicate the threshold energy of the dissociation continua corresponding to $H(1) + H(1)$, $H(1) + H(2)$, and $H(1) + H(3)$.

incomplete convergence only, and the estimated stabilization points are on the real axis). In the $b^3\Sigma_u^+$ block, however, we find no states below the $H(1) + H(1)$ continuum, in agreement with the BO calculations.⁷⁰ The next, $H(1) + H(2)$ threshold corresponds to the energy value $-0.624\,659\,800\,E_h$. Beyond the $H(1) + H(1)$ but below the $H(1) + H(2)$ thresholds stabilization points (with respect to the θ rotation angle and the basis set) were observed with small negative imaginary values, which were assigned (based on the real parts of the eigenvalues) to rotational–vibrational levels corresponding to the electronically excited states in their symmetry blocks (see Figure 4 and also Figure 3). The lack of any stabilization points beyond the $H(1) + H(2)$ threshold can be explained with the limited size and flexibility of the basis set.

It can be observed in Figure 4 in the $b^3\Sigma_u^+$ block that a group of stabilization points appear for $N = 1$ and 2 , which are not present for $N = 0$. These points for $N = 1$ and 2 were assigned to the rotational–vibrational states with $R = 0$ and 1 rotational angular momentum quantum numbers of the $c^3\Pi_u^+$ electronic state, respectively. This result demonstrates that the coupling of the rotational and orbital angular momenta is automatically included in the calculations by specifying only the total spatial angular momentum quantum number, N .

Finally, we note that the $H(1) + H(1)$ continuum does not couple neither to the “ $B^1\Sigma_u^+$ block” nor to the “ $a^3\Sigma_g^+$ block”, and in these cases the lowest-lying continuum corresponds to the $H(1) + H(2)$ dissociation channel (Figure 3).

Numerical Results for the Resonance Energies and Widths. In Table 4 numerical results are given for the

Table 4. Identified Resonance-State Energies and Widths, in E_h , of H_2 in the $b^3\Sigma_u^+$ Block [$p = (-1)^N$, $S_p = (1 + p)/2$, $S_e = 1$] for $N = 0, 1$, and 2

| $(N, p, S_p, S_e)^a$ | $\text{Re}(\mathcal{E})^b$ | $\Gamma/2^b$ | $E_{\text{ref,exp}}^c$ | $E_{\text{ref,theo}}^d$ | assignment ^e |
|----------------------|-----------------------------|----------------------|------------------------|----------------------------|---------------------------------------|
| (0,+1,1,1) | [−0.999 450 1] ^f | | | [−0.999 455 7] | H(1) + H(1) continuum |
| | [...] | | | | |
| (0,+1,1,1) | −0.677 947 1 | 1×10^{-7} | −0.677 946 1 | −0.677 942 7 ⁷⁰ | $e^3\Sigma_u^+$, $R = 0$, $\nu = 0$ |
| (0,+1,1,1) | −0.668 549 3 | 9×10^{-7} | −0.668 547 8 | −0.668 541 0 ⁷⁰ | $e^3\Sigma_u^+$, $R = 0$, $\nu = 1$ |
| (1,−1,0,1) | [−0.999 445 8] ^f | | | [−0.999 455 7] | H(1) + H(1) continuum |
| | [...] | | | | |
| (1,−1,0,1) | −0.731 434 0 | 5×10^{-7} | −0.731 438 8 | −0.731 469 1 ⁸² | $c^3\Pi_u^+$, $R = 0$, $\nu = 0$ |
| (1,−1,0,1) | −0.720 72 | 2×10^{-7} | −0.720 782 6 | | $c^3\Pi_u^+$, $R = 0$, $\nu = 1$ |
| | [...] | | | | |
| (1,−1,0,1) | −0.677 705 5 | 2×10^{-7} | −0.677 704 1 | −0.677 698 2 ⁷⁰ | $e^3\Sigma_u^+$, $R = 1$, $\nu = 0$ |
| (1,−1,0,1) | −0.668 32 | 1×10^{-6} | −0.668 319 7 | −0.668 309 8 ⁷⁰ | $e^3\Sigma_u^+$, $R = 1$, $\nu = 1$ |
| (2,+1,1,1) | [−0.999 439 7] ^f | | | [−0.999 455 7] | H(1) + H(1) continuum |
| | [...] | | | | |
| (2,+1,1,1) | −0.730 888 2 | 9×10^{-7} | −0.730 888 7 | | $c^3\Pi_u^+$, $R = 1$, $\nu = 0$ |
| (2,+1,1,1) | −0.720 219 0 | $< 2 \times 10^{-7}$ | −0.720 258 0 | | $c^3\Pi_u^+$, $R = 1$, $\nu = 1$ |
| | [...] | | | | |
| (2,+1,1,1) | −0.677 222 9 | 2×10^{-8} | −0.677 222 2 | | $e^3\Sigma_u^+$, $R = 2$, $\nu = 0$ |
| (2,+1,1,1) | −0.667 863 2 | 7×10^{-7} | −0.667 865 3 | | $e^3\Sigma_u^+$, $R = 2$, $\nu = 1$ |

^a N : total spatial angular momentum quantum number; p : parity, $p = (-1)^N$; S_p and S_e : total spin quantum numbers for the protons and electrons, respectively. ^b $\text{Re}(\mathcal{E})$ and Γ : resonance energy and width with $\Gamma/2 = -\text{Im}(\mathcal{E})$ calculated in this work. The largest basis set contained 15 500 basis functions for each set of quantum numbers. The proton–electron ratio was $m_p/m_e = 1836.152\,672\,47$.⁷¹ ^c $E_{\text{ref,exp}}$ experimental reference value, in E_h , derived as $E_{\text{exp}} = E_0 + T_{\text{exp}}$ with the ground-state energy ($X^1\Sigma_g^+$, $N = 0$, $\nu = 0$) $E_0 = -1.164\,025\,030\,E_h$. All T_{exp} values were obtained by correcting the experimental term values of Dieke,⁸¹ with $-0.000\,681\,7\,E_h = -149.63\,\text{cm}^{-1}$ ($1\,E_h = 219\,474.631\,4\,\text{cm}^{-1}$), since all triplet term values were too high.^{70,90} ^d $E_{\text{ref,theo}}$: the best available theoretical reference energy values, in E_h , corresponding to accurate adiabatic calculations for the $e^3\Sigma_u^+$ levels⁷⁰ and to accurate Born–Oppenheimer calculations for the $c^3\Pi_u^+$ levels.⁸² The nonrelativistic energy of two ground-state hydrogen atoms is given in square brackets. ^eBorn–Oppenheimer electronic- and vibrational-state labels. The (approximate) rotational angular momentum quantum number, R , is also given. ^fThe lowest-energy eigenvalue of the real Hamiltonian obtained with the largest parameter set and with the given quantum numbers.

“ $b^3\Sigma_u^+$ block”, B4, for the lowest-lying rotational–vibrational levels with $N = 0, 1$, and 2 corresponding to the $e^3\Sigma_u^+$ ($N = 0, 1, 2$) and to the $c^3\Pi_u^+$ ($N = 1, 2$) electronic-state labels. These rovibronic levels are embedded in the H(1) + H(1) continuum, and thus they are considered as rovibronic resonances.

The real energy values are in satisfactory agreement with the experimental results.⁸¹ We consider however the given imaginary parts as estimates to their accurate values, and all we can conclude at this point is that the obtained imaginary parts are of the order of $10^{-7}\,E_h$, which corresponds to a predissociative lifetime, $\tau = \hbar/\Gamma$, of the order of 0.2 ns. As it was explained earlier, it is difficult to assess the accuracy of the calculated resonance energies and widths since there is no such simple criterion as the (real) variational principle for bound states. According to our observations in the test calculations for Ps^- (Table 1), the relative errors in the real and imaginary parts with respect to the absolute value of the complex energy are similar. The accuracy of the pre-BO real energy values can be estimated here by their comparison with available experimental results. This observation also indicates that the resonance widths given in Table 4 should be considered as rough estimates.

Theoretical energy values are available in the literature calculated by Kolos and Rychlewski^{70,82} and are also cited in Table 4. In ref 70 adiabatic rotational–vibrational energy levels were determined for the $e^3\Sigma_u^+$ electronic state by calculating an accurate adiabatic potential energy curve and solving the corresponding rotational–vibrational Schrödinger equation. The theoretical reference value for the $c^3\Pi_u^+$, $R = 0$, $\nu = 0$ level was taken from ref 82, which was obtained by the calculation of an accurate BO potential energy curve and

solving the corresponding vibrational Schrödinger equation. The resulting BO energy could be furthermore corrected for the Λ -doubling, but the numerical value for this correction term was not clearly identifiable in ref 82. It would be interesting to see if nonadiabatic corrections can be calculated to these levels, for example using the recently developed nonadiabatic perturbation theory by Pachucki and Komasa.^{72,83}

The lifetimes of rotational–vibrational levels corresponding to the $e^3\Sigma_u^+$ state were measured in delayed coincidence experiments,⁸⁴ which include both the radiative and predissociative decay channels accessible from these levels. In the same work the competition of the two decay channels was investigated using ab initio (full configuration interaction electronic wave functions using Gaussian-type orbitals and an accurate adiabatic potential energy curve⁷⁰) as well as quantum defect theory with a one-channel approximation.⁸⁴ According to these calculations the predissociative lifetimes are of the order of 1 μs and 100 ns for the $\nu = 0$ and $\nu = 1$ vibrational levels, respectively, for the $e^3\Sigma_u^+$ state with $N = 0$. The lifetimes of the lowest rotational–vibrational levels of the $c^3\Pi_u^+$ state were calculated using a simple perturbative model, which included the orbit–rotation interaction and used several approximations during the calculations.⁸⁵ In a similar perturbative treatment,⁸⁶ the orbit–rotational coupling operator was included, and accurate BO potential energy curves were used to describe the $b^3\Sigma_u^+$ and $c^3\Pi_u^+$ states.^{82,87} According to both the lifetime measurements^{88,89} and the calculations^{85,86} the predissociative lifetime of the lowest-lying rotational–vibrational levels of $c^3\Pi_u^+$ is of the order of 1 ns. Unfortunately, calculated energy levels were not reported in any of these theoretical works^{84–86} on the predissociative

lifetimes of the $e^3\sum_u^+$ and $c^3\Pi_u^+$ states, which makes comparison of the results more difficult.

To pinpoint the resonance energies and especially the widths of the rovibronic levels within the rigorous pre-BO framework developed in the present work, further calculations are necessary. Nevertheless, the results shown in Table 4 improve on the best available theoretical values for energy levels published in the literature.^{70,82} Furthermore, our primary goal was also completed, as it was demonstrated that in pre-BO calculations (a) electronically excited rovibronic levels are accessible and (b) there are excited rovibronic levels, which are described as bound states in the BO theory but appear as resonances in a pre-BO description, i.e., if the introduction of the BO approximation is completely avoided.

How to Improve on the Present Results? First of all, one of the lessons of the present study is that an efficient parametrization of the basis set is one of the main challenges of the calculation of rovibronic resonances in pre-BO theory.

We have shown that the random generation of parameters can be improved using the parameter-transfer approach assuming that there are bound states of comparable internal structure to the quasi-bound states to be calculated. In the case of H_2 the presented calculations could be improved by the tight optimization of parameter sets for the lowest-lying bound states with unnatural parity, $p = (-1)^{N+1}$, and by the inclusion of also these parameters in an extended parameter set.

Then another technically straightforward, but computationally more demanding, option is the optimization of parameters not only for the lowest-lying states of a symmetry block but also for more (or all) vibrational and vibronic excited bound states, e.g., for all (ro)vibrational states of $X^1\Sigma_g^+$ up to the $H(1) + H(1)$ threshold or for all the bound (ro)vibronic energy levels corresponding to the " $B^1\Sigma_u^+$ block" as well as to the " $a^3\Sigma_g^+$ block" up to their lowest-lying correlating threshold, $H(1) + H(2)$ (see Figure 3).

Finally, a more generally applicable solution to the parametrization problem of resonance states would be the development of a useful and practical application of the complex variational principle for resonances.²⁴

SUMMARY AND OUTLOOK

The present work was devoted to the calculation of rotational–vibrational energy levels corresponding to electronically excited states, which are bound within the Born–Oppenheimer (BO) approximation but appear as resonances in a pre-Born–Oppenheimer (pre-BO) quantum mechanical description.

To calculate resonance energies and widths, corresponding to predissociative lifetimes, the pre-BO variational approach and computer program of ref 44 were extended with the complex coordinate rotation method (CCRM). Similarly to the bound-state calculations, the wave function was written as a linear combination of basis functions which have the non-relativistic quantum numbers (total spatial–rotational plus orbital–angular momentum quantum number, parity, and total spin quantum number for each particle type). The basis functions were constructed using explicitly correlated Gaussian functions and the global vector representation.

This pre-BO resonance approach was first used for the three- and four-particle positronium complexes, $Ps^- = \{e^-, e^-, e^+\}$ and $Ps_2 = \{e^-, e^-, e^+, e^+\}$, respectively. These applications allowed us to test the implementation and gain experience in the identification of resonance parameters. For the dipositronium,

Ps_2 , we managed to improve on some of the best available results reported in the literature.

Then, the developed methodology and technology was employed for the four-particle molecule, H_2 . First, the rovibronic states known in the literature were collected and considered which were accessible in our calculations with various sets of (exact) quantum numbers of the nonrelativistic theory. The experimental and theoretical energy values of the literature were also used for the assignment of our calculated energy levels with the common BO terminology of electronic and vibrational state labels.

As to the computational part, we had to find a useful parametrization strategy for the basis functions. Since the bound-state parameter-optimization approach relied on the energy minimization condition and the (real) variational principle, it was not directly applicable for making the CCRM calculations more efficient. A simple and practical solution to the parametrization problem was the parameter-transfer approach, where the basis functions used to describe low-energy resonances of some symmetry were parametrized with optimized parameters of (high-energy) bound states. As a result, a large parameter set was constructed, which was compiled from parameters optimized for different symmetry blocks. The parametrization of basis functions, which have mathematical forms defined by the exact quantum numbers, with this extended parameter set immediately lead to an improvement for the best available energy values available in the literature for the lowest-lying rotational states assigned to the $B^1\Sigma_u^+$ and $a^3\Sigma_g^+$ electronic states.

Then, using this extended parameter set low-energy rovibronic resonances became accessible beyond the $b^3\Sigma_u^+$ repulsive electronic state, embedded in the $H(1) + H(1)$ continuum. On the basis of these calculations, resonance energies were evaluated, and resonance widths were estimated for the lowest-lying rotational–vibrational levels of the electronically excited $e^3\sum_u^+$ and $c^3\Pi_u^+$ states. We note here that the coupling of the rotational and orbital angular momenta was automatically included in our computational approach by specifying only the total spatial angular momentum quantum number, N . Although the presented results improve on the best available (BO and adiabatic) calculations in the literature for these states, to pinpoint the resonance energies and especially the widths more extensive calculations are necessary.

As for further improvements, the major present technical difficulty is the efficient parametrization of the basis set for resonance states. A generally applicable solution to this problem would be a useful application and implementation of a complex analogue for the real variational principle. In the lack of such a general solution, optimization of large parameter sets for bound (excited) states together with the parameter-transfer strategy might be appropriate for the calculation of a larger number and/or more accurate rovibronic resonances of H_2 . In addition to the improvement of the parametrization strategy, a generally applicable analysis tool would also be desirable which provides an assignment for the pre-BO wave function with the common BO electronic- and vibrational-state labels where such an assignment is possible.

ASSOCIATED CONTENT

Supporting Information

Additional experimental details. This material is available free of charge via the Internet at <http://pubs.acs.org>.

■ AUTHOR INFORMATION

Corresponding Author

*E-mail: matyus@chem.elte.hu.

Notes

The authors declare no competing financial interest.

■ ACKNOWLEDGMENTS

E.M. is thankful to Prof. Attila G. Császár and Prof. Markus Reiher for the continuous encouragement and also thanks Benjamin Simmen for discussions. The financial support of the Hungarian Scientific Research Fund (OTKA, NK83583) and an ERA-Chemistry grant is gratefully acknowledged. The computing facilities of HPC-Debrecen (NIIFI) were used during this work.

■ REFERENCES

- (1) Born, M.; Oppenheimer, R. Zur Quantentheorie der Molekeln. *Ann. der Phys.* **1927**, *84*, 457–484.
- (2) Born, M. Kopplung der Elektronen- und Kernbewegung in Molekeln und Kristallen. *Nachr. Akad. Wiss. Göttingen, Math.-Phys. Kl.*, **2** **1951**, *6*, 1–3.
- (3) Born, M.; Huang, K. *Dynamical Theory of Crystal Lattices*; Clarendon Press: Oxford, 1954.
- (4) Woolley, R. G. Quantum Theory and Molecular Structure. *Adv. Phys.* **1976**, *25*, 27–52.
- (5) Woolley, R. G. Most a Molecule Have a Shape? *J. Am. Chem. Soc.* **1978**, *100*, 1073–1078.
- (6) Woolley, R. G.; Sutcliffe, B. T. Molecular Structure and the Born–Oppenheimer Approximation. *Chem. Phys. Lett.* **1977**, *45*, 393–398.
- (7) Weininger, S. J. The Molecular Structure Conundrum: Can Classical Chemistry Be Reduced to Quantum Chemistry? *J. Chem. Educ.* **1984**, *61*, 939–944.
- (8) Claverie, P.; Diner, S. The Concept of Molecular Structure in Quantum Theory: Interpretation Problems. *Isr. J. Chem.* **1980**, *19*, 54–81.
- (9) Woolley, R. G. Quantum Mechanical Aspects of the Molecular Structure Hypothesis. *Isr. J. Chem.* **1980**, *19*, 30–46.
- (10) Woolley, R. G. Molecular Shapes and Molecular Structures. *Chem. Phys. Lett.* **1986**, *125*, 200–205.
- (11) Cafiero, M.; Adamowicz, L. Molecular Structure in Non-Born–Oppenheimer Quantum Mechanics. *Chem. Phys. Lett.* **2004**, *387*, 136–141.
- (12) Sutcliffe, B. T.; Woolley, R. G. Comment on ‘Molecular Structure in Non-Born–Oppenheimer Quantum Mechanics’. *Chem. Phys. Lett.* **2005**, *408*, 445–447.
- (13) Müller-Herold, U. On the Emergence of Molecular Structure from Atomic Shape in the $1/r^2$ Harmonium Model. *J. Chem. Phys.* **2006**, *124*, 014105-1–5.
- (14) Müller-Herold, U. On the Transition Between Directed Bonding and Helium-Like Correlation in a Modified Hooke–Calogero Model. *Eur. Phys. J. D* **2008**, *49*, 311–315.
- (15) Ludeña, E. V.; Echevarra, L.; Lopez, X.; Ugalde, J. M. Non-Born–Oppenheimer Electronic and Nuclear Densities for a Hooke–Calogero Three-Particle Model: Non-Uniqueness of Density-Derived Molecular Structure. *J. Chem. Phys.* **2012**, *136*, 084103-1–12.
- (16) Cassam-Chenai, P. A Mathematical Definition of Molecular Structure – Open Problem. *J. Math. Chem.* **1998**, *23*, 61–63.
- (17) Goli, M.; Shahbazian, S. Atoms in Molecules: Beyond Born–Oppenheimer Paradigm. *Theor. Chim. Acta* **2011**, *129*, 235–245.
- (18) Goli, M.; Shahbazian, S. The Two-Component Quantum Theory of Atoms in Molecules (TC-QTAIM): Foundations. *Theor. Chim. Acta* **2012**, *131*, 1208-1–19.
- (19) Mátyus, E.; Hutter, J.; Müller-Herold, U.; Reiher, M. On the Emergence of Molecular Structure. *Phys. Rev. A* **2011**, *83*, 052512-1–5.
- (20) Mátyus, E.; Hutter, J.; Müller-Herold, U.; Reiher, M. Extracting Elements of Molecular Structure from the All-Particle Wave Function. *J. Chem. Phys.* **2011**, *135*, 204302-1–12.
- (21) Harris, R. A. Predissociation. *J. Chem. Phys.* **1963**, *39*, 978–987.
- (22) Kukulin, V. I.; Krasnopolsky, V. M.; Horáček, J. *Theory of Resonances—Principles and Applications*; Kluwer: Dordrecht, 1988.
- (23) Reinhardt, W. P. Complex Coordinates in the Theory of Atomic and Molecular Structure and Dynamics. *Annu. Rev. Phys. Chem.* **1982**, *33*, 223–255.
- (24) Moiseyev, N. Quantum Theory of Resonances: Calculating Energies, Widths and Cross-Sections by Complex Scaling. *Phys. Rep.* **1998**, *302*, 211.
- (25) Hazi, A. U.; Taylor, H. S. Stabilization Method of Calculating Resonance Energies: Model Problem. *Phys. Rev. A* **1970**, *1*, 1109–1120.
- (26) Ho, Y. K. *The Method of Complex Coordinate Rotation and its Applications to Atomic Collision Processes*; North-Holland Publishing Company: Amsterdam, 1983.
- (27) Usukura, J.; Suzuki, Y. Resonances of Positronium Complexes. *Phys. Rev. A* **2002**, *66*, 010502(R)-1–4.
- (28) Mandelshtam, V. A.; Ravuri, T. R.; Taylor, H. S. Calculation of the Density of Resonance States Using the Stabilization Method. *Phys. Rev. Lett.* **1993**, *70*, 1932–1935.
- (29) Mandelshtam, V. A.; Taylor, H. S.; Ryaboy, V.; Moiseyev, N. Stabilization Theory for Computing Energies and Widths of Resonances. *Phys. Rev. A* **1994**, *50*, 2764–2766.
- (30) Müller, J.; Yang, X.; Burgdörfer, J. Calculation of Resonances in Doubly Excited Helium Using the Stabilization Method. *Phys. Rev. A* **1994**, *49*, 2470–2475.
- (31) Ryaboy, V.; Moiseyev, N.; Mandelshtam, V. A.; Taylor, H. S. Resonance Positions and Widths by Complex Scaling and Modified Stabilization Method: van der Waals Complex $\text{NeI} \cdot \text{Cl}$. *J. Chem. Phys.* **1994**, *101*, 5677–5682.
- (32) Aguilar, J.; Combes, J. M. A Class of Analytic Perturbations for One-Body Schrödinger Hamiltonians. *Commun. Math. Phys.* **1971**, *22*, 269–279.
- (33) Balslev, E.; Combes, J. M. Spectral Properties of Many-Body Schrödinger Operators with Dilatation-Analytic Interactions. *Commun. Math. Phys.* **1971**, *22*, 280–294.
- (34) Simon, B. Quadratic Form Techniques and the Balslev–Combes Theorem. *Commun. Math. Phys.* **1972**, *27*, 1–9.
- (35) Wang, D.; Bowman, J. M. Complex L^2 Calculations of Bound States and Resonances of HCO and DCO. *Chem. Phys. Lett.* **1995**, *235*, 277–285.
- (36) Rom, N.; Engdahl, E.; Moiseyev, N. Tunneling Rates in Bound Systems Using Smooth Exterior Complex Scaling within the Framework of the Finite Basis Set Approximation. *J. Chem. Phys.* **1990**, *93*, 3413–3419.
- (37) Rom, N.; Lipkin, N.; Moiseyev, N. Optical Potentials by the Complex Coordinate Method. *Chem. Phys.* **1991**, *151*, 199–204.
- (38) Riss, U. V.; Meyer, H.-D. Calculation of Resonance Energies and Widths Using the Complex Absorbing Potential Method. *J. Phys. B* **1993**, *26*, 4503–4536.
- (39) Seideman, T.; Miller, W. H. Calculation of the Cumulative Reaction Probability via a Discrete Variable Representation with Absorbing Boundary Conditions. *J. Chem. Phys.* **1992**, *96*, 4412–4422.
- (40) Thompson, W. H.; Miller, W. H. On the “Direct” Calculation of Thermal Rate Constants. II. The Flux-Flux Autocorrelation Function with Absorbing Potentials, with Application to the $\text{O} + \text{HCl} \rightarrow \text{OH} + \text{Cl}$ Reaction. *J. Chem. Phys.* **1997**, *106*, 142–150.
- (41) Miller, W. H. “Direct” and “Correct” Calculation of Canonical and Microcanonical Rate Constants for Chemical Reactions. *J. Phys. Chem. A* **1998**, *102*, 793–806.
- (42) Papp, Z.; Darai, J.; Nishimura, A.; Hlousek, Z. T.; Hu, C.-Y.; Yakovlev, S. L. Faddeev–Merkuriev Equations for Resonances in Three-Body Coulombic Systems. *Phys. Lett. A* **2002**, *304*, 36–42.
- (43) Papp, Z.; Darai, J.; Mezei, J. Z.; Hlousek, Z. T.; Hu, C.-Y. Accumulation of Three-Body Resonances above Two-Body Thresholds. *Phys. Rev. Lett.* **2005**, *94*, 143201-1–4.

- (44) Mátyus, E.; Reiher, M. Molecular Structure Calculations: a Unified Quantum Mechanical Description of Electrons and Nuclei using Explicitly Correlated Gaussian Functions and the Global Vector Representation. *J. Chem. Phys.* **2012**, *137*, 024104–1–17.
- (45) Simmen, B.; Mátyus, E.; Reiher, M. Elimination of the Translational Kinetic Energy Contamination in Pre-Born–Oppenheimer Calculations. *Mol. Phys.* **2013**, DOI: 10.1080/00268976.2013.783938.
- (46) Cohen, E.; Cvitaš, T.; Frey, J.; Holmström, B.; Kuchitsu, K.; Marquardt, R.; Mills, I.; Pavese, F.; Quack, M.; Stohner, J.; et al. *Quantities, Units and Symbols in Physical Chemistry (the IUPAC Green Book - 3rd ed.)*; RSC Publishing: Cambridge, 2007.
- (47) Boys, S. F. The Integral Formulae for the Variational Solution of the Molecular Many-Electron Wave Equation in Terms of Gaussian Functions with Direct Electronic Correlation. *Proc. R. Soc. London A* **1960**, *369*, 402–411.
- (48) Singer, K. The Use of Gaussian (Exponential Quadratic) Wave Functions on Molecular Problems I. General Formulae for the Evaluation of Integrals. *Proc. R. Soc. London A* **1960**, *258*, 412–420.
- (49) Jeziorski, B.; Szalewicz, K. High-Accuracy Compton Profile of Molecular Hydrogen from Explicitly Correlated Gaussian Wave Function. *Phys. Rev. A* **1979**, *19*, 2360–2365.
- (50) Cencek, W.; Rychlewski, J. Many-Electron Explicitly Correlated Gaussian Functions. I. General Theory and Test Results. *J. Chem. Phys.* **1993**, *98*, 1252–1261.
- (51) Rychlewski, J., Ed. *Explicitly Correlated Wave Functions in Chemistry and Physics*; Kluwer Academic Publishers: Dordrecht, 2003.
- (52) Suzuki, Y.; Usukura, J.; Varga, K. New Description of Orbital Motion with Arbitrary Angular Momenta. *J. Phys. B: Atmos. Mol. Opt. Phys.* **1998**, *31*, 31–48.
- (53) Varga, K.; Suzuki, Y.; Usukura, J. Global-Vector Representation of the Angular Motion of Few-Particle Systems. *Few-Body Systems* **1998**, *24*, 81–86.
- (54) Suzuki, Y.; Varga, K. *Stochastic Variational Approach to Quantum-Mechanical Few-Body Problems*; Springer-Verlag: Berlin, 1998.
- (55) Schrader, D. M. Symmetry of Dipositronium, Ps_2 . *Phys. Rev. Lett.* **2004**, *92*, 043401–1–4.
- (56) Schrader, D. M. Symmetries and States of Ps_2 . *Nucl. Instrum. Methods Phys. Res., Sect. B* **2004**, *221*, 182–184.
- (57) Schrader, D. M. General Forms of Wave Functions for Dipositronium, Ps_2 . In *NASA GSFC Science Symposium on Atomic and Molecular Physics*; Bhatia, A. K., Ed.; NASA/CP-2006–214146, Goddard Space Flight Center: Greenbelt, MD, 2007; pp 103–110.
- (58) Anderson, E.; Bai, Z.; Bischof, C.; Blackford, S.; Demmel, J.; Dongarra, J.; Du Croz, J.; Greenbaum, A.; Hammarling, S.; McKenney, A.; et al. *LAPACK Users' Guide*, 3rd ed.; Society for Industrial and Applied Mathematics: Philadelphia, PA, 1999.
- (59) Kukulin, V. I.; Krasnopol'sky, V. M. A Stochastic Variational Method for Few-Body Systems. *J. Phys. G: Nucl. Phys.* **1977**, *3*, 795–811.
- (60) Alexander, S. A.; Monkhorst, H. J.; Szalewicz, K. Random Tempering of Gaussian-Type Geminals. I. Atomic Systems. *J. Chem. Phys.* **1986**, *85*, 5821–5825.
- (61) Alexander, S. A.; Monkhorst, H. J.; Szalewicz, K. Random Tempering of Gaussian-Type Geminals. II. Molecular Systems. *J. Chem. Phys.* **1987**, *87*, 3976–3980.
- (62) Alexander, S. A.; Monkhorst, H. J.; Szalewicz, K. Random Tempering of Gaussian-Type Geminals. III. Coupled Pair Calculations on Lithium Hydride and Beryllium. *J. Chem. Phys.* **1988**, *89*, 355–359.
- (63) Powell, M. J. D. The NEWUOA software for unconstrained optimization without derivatives (DAMTP 2004/NA05), Report no. NA2004/08, <http://www.damtp.cam.ac.uk/user/na/reports04.html> (accessed on January 18, 2013).
- (64) Li, T.; Shakeshaft, R. S-Wave Resonances of the Negative Positronium Ion and Stability of a Systems of Two Electrons and an Arbitrary Positive Charge. *Phys. Rev. A* **2005**, *71*, 052505–1–7.
- (65) Suzuki, Y.; Usukura, J. Stochastic Variational Approach to Resonances of Ps^- and Ps_2 . *Nucl. Instrum. Methods Phys. Res., Sect. B* **2004**, *221*, 195–199.
- (66) Korobov, V. I. Coulomb Three-Body Bound-State Problem: Variational Calculations of Nonrelativistic Energies. *Phys. Rev. A* **2000**, *61*, 064503–1–3.
- (67) DiRienzi, J.; Drachman, R. J. Resonances in the Dipositronium System: Rydberg States. *Can. J. Phys.* **2010**, *88*, 877–883.
- (68) Suzuki, Y.; Usukura, J. Excited States of the Positronium Molecule. *Nucl. Instrum. Methods Phys. Res., Sect. B* **2000**, *171*, 67–80.
- (69) Bubin, S.; Adamowicz, L. Nonrelativistic Variational Calculations of the Positronium Molecule and the Positronium Hydride. *Phys. Rev. A* **2006**, *74*, 052502–1–5.
- (70) Kolos, W.; Rychlewski, J. Adiabatic Potential Energy Curves for the b and $e^3\Sigma_u^+$ States of the Hydrogen Molecule. *J. Mol. Spectrosc.* **1990**, *143*, 237–250.
- (71) <http://physics.nist.gov/cuu/Constants> (CODATA 2006).
- (72) Pachucki, K.; Komasa, J. Nonadiabatic Corrections to Rovibrational Levels of H_2 . *J. Chem. Phys.* **2009**, *130*, 164113–1–11.
- (73) Wolniewicz, L.; Orlikowski, T.; Staszewska, G. $^1\Sigma_u$ and $^1\Pi_u$ States of the Hydrogen Molecule: Nonadiabatic Couplings and Vibrational Levels. *J. Mol. Spectrosc.* **2006**, *238*, 118–126.
- (74) Wolniewicz, L.; Dressler, K. Nonadiabatic Energy Corrections for the Vibrational Levels of the B and $B'^1\Sigma_u^+$ States of the H_2 and D_2 Molecules. *J. Chem. Phys.* **1992**, *96*, 6053–6064.
- (75) Wolniewicz, L. Lowest Order Relativistic Corrections to the Energies of the $B^1\Sigma_u$ State of H_2 . *Chem. Phys. Lett.* **1995**, *233*, 647–650.
- (76) Dressler, K.; Wolniewicz, L. Experiment and Theory of High Resolution Spectra of Rovibronic Molecular States. *Ber. Bunsenges. Phys. Chem.* **1995**, *99*, 246–250.
- (77) Wolniewicz, L. Non-Adiabatic Energies of the $a^3\Sigma_g^+$ State of the Hydrogen Molecule. *Mol. Phys.* **2007**, *105*, 1497–1503.
- (78) Herzberg, G. *Spectra of Diatomic Molecules*; D. Van Nostrand Company, Inc.: Princeton, NJ, 1950.
- (79) Brown, J.; Carrington, A. *Rotational Spectroscopy of Diatomic Molecules*; Cambridge University Press: Cambridge, 2003.
- (80) The term “spectroscopic accuracy” is not uniquely defined, but it is usually used to refer to calculations providing vibrational transition wave numbers with a certainty of at least 1 cm^{-1} ($\approx 4.6\text{ }\mu\text{E}_h$) and even better accuracy for calculated rotational transitions.
- (81) Dieke, G. H. The Molecular Spectrum of Hydrogen and Its Isotopes. *J. Mol. Spectrosc.* **1958**, *2*, 494–517.
- (82) Kolos, W.; Rychlewski, J. Ab initio Potential Energy Curves and Vibrational Levels for the c , I , and i States of the Hydrogen Molecule. *J. Mol. Spectrosc.* **1977**, *66*, 428–440.
- (83) Pachucki, K.; Komasa, J. Nonadiabatic Corrections to the Wave Function and Energy. *J. Chem. Phys.* **2008**, *129*, 034102–1–7.
- (84) Kiyoshima, T.; Sato, S.; Adamson, S. O.; Pazyuk, E. A.; Stolyarov, A. V. Competition Between Predissociative and Radiative Decays in the $e^3\Sigma_u^+$ and $d^3\Pi_u^-$ States of H_2 and D_2 . *Phys. Rev. A* **1999**, *60*, 4494–4502.
- (85) Chiu, L.-Y. C.; Bhattacharyya, D. K. Lifetimes of Fine Structure Levels of Metastable H_2 in the $c^3\Pi_u$ State. *J. Chem. Phys.* **1979**, *70*, 4376–4382.
- (86) Comtet, G.; de Bruijn, D. P. Calculation of the Lifetimes of Predissociative Levels of the $c^3\Pi_u$ State in H_2 , HD and D_2 . *Chem. Phys.* **1985**, *94*, 365–370.
- (87) Kolos, W.; Wolniewicz, L. Potential-Energy Curves for the $X^1\Sigma_g^+$, $b^3\Sigma_u^+$ and $C^3\Pi_u$ States of the Hydrogen Molecule. *J. Chem. Phys.* **1965**, *43*, 2429–2441.
- (88) Meierjohann, B.; Vogler, M. Vibrationally Resolved Predissociation of the $C^3\Pi_u$ and $e^3\Sigma_u^+$ States of H_2 by Flight-Time-Difference Spectroscopy. *Phys. Rev. A* **1978**, *17*, 47–51.
- (89) de Bruijn, D. P.; Neuteboom, J.; Los, J. Predissociation of the $C^3\Pi_u$ State of H_2 , Populated after Charge Exchange of H_2^+ with Several Targets at keV Energies. *Chem. Phys.* **1984**, *85*, 233–251.

(90) Miller, T. A.; Freund, R. S. Singlet-Triplet Anticrossings in H_2 . *J. Chem. Phys.* **1974**, *61*, 2160–2162.